

NOVEL SYNTHESIS OF GOLD DOPED SILVER PHOSPHATE NANOPARTICLES BY HYDROTHERMAL METHOD FOR THE ENHANCEMENT OF VISIBLE LIGHT-RESPONSIVE PHOTOCATALYTIC DEGRADATION OF FAST GREEN FCF DYE

Amin K. Qasim^a^aDept. of Environmental Sciences, Faculty of Science, University of Zakho, Kurdistan Region, Iraq. (Amin.qasim@uoz.edu.krd)**Received:** 04 Apr., 2022 / **Accepted:** 04 Jun., 2022 / **Published:** 01 Jul., 2022<https://doi.org/10.25271/sjuoz.2022.10.3.916>**ABSTRACT:**

In this study, the gold (Au) noble metal doped Ag₃PO₄ nanoparticles (NPs) were synthesized by hydrothermal method. The obtained photocatalysts NPs were characterized via FE-SEM, EDX, XRD and UV-Vis spectrophotometer. The crystal structure and phase were identified by XRD characterization. From the XRD the structure of Ag₃PO₄ NPs was not altered after doping with Au as a noble metal; in addition the sharp and narrow peaks indicate that Ag₃PO₄ NPs are high purity and have a crystalline structure. And the XRD pattern of samples after doping indicates that Au distributed homogeneously in Ag₃PO₄. The morphology of bare Ag₃PO₄ and Au doped Ag₃PO₄ were studied by FE-SEM. The average sizes of the synthesized Ag₃PO₄ and Au doped Ag₃PO₄ NPs were 747.81 nm and 96.77nm respectively. EDX is utilized for the elemental composition analysis of the synthesized NPs and the pattern consists of corresponding peaks for P, Ag, O, and Au ions and it confirms the doped of Au noble metal ion in the prepared samples. The optical properties and the band gap were estimated by UV-Vis spectrophotometer. The band gap was found for undoped and doped Ag₃PO₄ NPs were 2.39 eV and 2.34 eV respectively. Furthermore, the photocatalytic performances for bare Ag₃PO₄ NPs and Au doped Ag₃PO₄ were studied with fast green FCF dye. As a result the Au@ Ag₃PO₄ could be considered the optimum photocatalyst because the target dye molecule is degraded in 15 min, in contrast the bare Ag₃PO₄ NPs needed 55min. The photo degradation rate of the Au@ Ag₃PO₄ NPs is ~3 times higher than the rate of Ag₃PO₄ NPs. Finally, Au@ Ag₃PO₄ NPs confirmed the highest photodegradation catalyst compared with other bare Ag₃PO₄ NPs.

KEYWORD: Au@Ag₃PO₄ NPs, hydrothermal method, fast green FCF dye, visible light and Photocatalyst.**1. INTRODUCTION**

Toxic chemicals and untreated waste, such as dyestuffs, herbicides, pesticides, and lab effluents, from agricultures, industries and other sources poses a major problem to wastewater sources through diffusion (Alam, Fleisch, Kretschmer, Bahnemann, & Muneer, 2017; Faisal et al., 2020; Faisal, Khan, et al., 2011a, 2011b; Farah, Ateeq, Ali, Sabir, & Ahmad, 2004). Due to serious environmental health problems and toxicity consequences are good reason for removing these dyestuff and wastes from wastewater (Dayana, Abel, Inbaraj, Sivaranjani, & Thiruneelakandan, 2021; Kumar, Gayathri, & Anthony, 2016; Long et al., 2009; Nagaraju, Shivaraju, Banuprakash, & Rangappa, 2017). Therefore, degradation of these dyestuff and other wastes by photocatalysts is highly favorable for the proper management of these highly toxic and unfavorable compounds (Bouid, Faisal, Harraz, Al-Sayari, & Ismail, 2015; Faisal, Khan, Rahman, Jamal, Akhtar, et al., 2011; Faisal, Tariq, & Muneer, 2007; Rawat, Bijalwan, Negi, Sharma, & Dwivedi, 2021).

Nowadays, many metals and metal oxide NPs Photocatalysts such as copper, zinc, titanium and nickel oxide have been synthesized (Karimi-Maleh et al., 2020). Among them a silver orthophosphate (Ag₃PO₄) semiconductor, reported by Yi and co-workers (Omer, 2008). Moreover, it has exhibited extremely high photo oxidative capabilities for O₂ evolution from water due to its highly positive valance band (VB) position (Guan & Guo, 2014), as well as organic dye decomposition under visible light irradiation, low-toxicity and high photocatalytic ability. In addition, as a unique one, Ag₃PO₄ is so far the only compound that incorporates nonmetallic p-block specie into Ag₂O (CHENG, LIU, Juan, & WANG, 2015). More importantly,

it possesses ultra-high photocatalytic activity in O₂ evolution and organic contaminant degradation (Yi et al., 2010).

In addition, still some inherent limitations in the present Ag₃PO₄ photocatalytic system. It is well known that Ag₃PO₄ is slightly soluble in aqueous solution, which greatly reduces its stability during the photocatalytic process (Atacan, Güy, Ozmen, & Özar, 2021; Rycenga et al., 2011) Thus, many efforts have been focused on to increase the photocatalytic activity and stability of Ag₃PO₄ during the degradation of organic dyes in aqueous solution.

Doping is an effective way to improve the properties of Ag₃PO₄ nanoparticles NPs, various types of extrinsic dopants, for instance, metal cations (Ilican, 2013) and non-metal anions (Anusha & Arivuoli, 2013; Downing, Ryan, & McLachlan, 2013; F. Wang et al., 2014) have been introduced into Ag₃PO₄ for enhancing the photocatalytic activity and stability. Recently; doping of noble metals (Ag, Au and Pd) in to semiconductor oxides to improve photocatalytic efficiency (Pathak, Swart, & Kroon, 2018). Furthermore, Noble metal Au incorporation with metal-oxide nanoparticles NPs is known to influence the structural properties due to different work functions and electron movement (Rawat et al., 2021). However, in plasmonic NPs photocatalysts, could increase the efficiency of absorb visible light by noble metals such as Au and act as a thermal redox-active site or as an electronic contractor for electron transfer during reactions (Sarina, Waclawik, & Zhu, 2013; P. Wang, Huang, Dai, & Whangbo, 2012). Fast green dye is a compound commonly used as food colorant by the cosmetics and drug industries (Okafor et al., 2016). However, fast green dye is highly toxic colorant having mutagenic, carcinogenic properties and possess significant threats to the human beings for example skin, eyes, respiratory tracts as well as aquatic life. Therefore, it is necessary destroy and degraded completely from

* This is an open access under a CC BY-NC-SA 4.0 license (<https://creativecommons.org/licenses/by-nc-sa/4.0/>)

industrial effluent to protect the ecosystem (Sharma, Bhogal, Naushad, Kumar, & Stadler, 2017). Different methods were used to synthesize Photocatalyst NPs, such as solvothermal (Kathirvel, Pedaballi, Su, Chen, & Li, 2020), precipitation (Wategaonkar et al., 2020), sol-gel (Vickers, 2017), and emulsion precipitation (Bauer & Tomandl, 1994). Herein, we have detailed the synthesis of Ag_3PO_4 NPs by hydrothermal method at certain temperature and their subsequent doping with Au to create Au- Ag_3PO_4 nanoparticles. However, the synthesized metal oxide NPs were characterized to explore their properties and utilized as a photocatalyst for the degradation of fast green FCF dye under ultraviolet and visible light irradiation.

2. MATERIAL AND METHODS

Silver nitrate (AgNO_3), sodium triphosphate ($\text{Na}_5\text{P}_3\text{O}_{10}$), fast green FCF dye, and sodium borohydride (NaBH_4) were obtained from Merck. Trichlorogold; hydrochloride ($\text{HAuCl}_4 \cdot x\text{H}_2\text{O}$) from Sigma Aldrich. Benzoquinone (BQ), disodium ethylenediaminetetraacetate ($\text{Na}_2\text{-EDTA}$) and tert-butanol (t-BuOH) from alpha. Double distilled water (DDW) is used as a solvent for the reaction.

2.1 Preparation of silver phosphate nanoparticles (Ag_3PO_4 NPs)

The synthesis method involves a little modified procedure reported by Keziban Atacan et al (Atacan, Özacar, & Özacar, 2018), for the preparation of Ag doped metal oxide NPs. Ag_3PO_4 NPs were synthesized by using a one-pot hydrothermal method in a 50 ml Teflon lined stainless steel autoclave. In a typical reaction, 0.2 g of AgNO_3 and 0.2 g of $\text{Na}_5\text{P}_3\text{O}_{10}$ (1:1) were dissolved in 30 mL of DD water under vigorous stirring for getting a homogenous mixture. Afterward stirred for about 20 min, mixture was transferred in teflon lined autoclave 50 ml and the autoclave was heated in an oven at 120°C for 12 h. After being cooled to room temperature, the obtained precipitate was collected by centrifugation, washed several times with DD water and then dried at 75°C in a vacuum oven for further use.

2.2 Preparation of Au doped silver phosphate nanoparticles (Au@ Ag_3PO_4 NPs)

Synthesis of Au-doped Ag_3PO_4 NPs, the chemical reduction method was preferred (Atacan et al., 2018). For the doping process, 0.5 g of Ag_3PO_4 NPs was dispersed in 40 mL of DD water under sonication for 15 min. Subsequently, 39.35 mg of Trichlorogold; hydrochloride ($\text{HAuCl}_4 \cdot x\text{H}_2\text{O}$) (calculated as 5% of the Ag_3PO_4 weight amount is Au) was added and stirred for 30 min. Then, 20 mL of NaBH_4 (0.0175 M) was dropped into the mixture and stirred for 1 h at room temperature to reduce Au^{3+} ions to metallic Au^0 onto Ag_3PO_4 NPs surface. The obtained Au@ Ag_3PO_4 NPs were centrifuged, washed with DD water, and dried at 70°C as shown in Fig (1).

2.3 Evaluation of Photocatalytic activity of Ag_3PO_4 NPs and Au@ Ag_3PO_4 NPs

A Photocatalytic activity of the catalyst was evaluated by degradation of fast green FCF dye under visible light irradiation. In a typical process, 100 mg of catalyst was dispersed in 100 ml of FG dye aqueous solution (10 mg/L), and then kept in the dark for 2 h, to establish adsorption and desorption equilibrium between FG dye and catalyst before irradiation. This was then irradiated with a 150W and 4200K (CDM, 942, G12) lamp. A solution of the degraded sample were taken at an interval of 2 min and centrifuged at 1000 rpm. The absorbance of supernatant was detected at λ_{max} of 625 nm. Also, the percentage of degradation of the dye molecules with respect to time is calculated by the following equation (Eq. 1)

$$n = 1 - \frac{C_t}{C_0} \times 100 \quad (1)$$

Where C_0 and C_t are the dye concentration at the beginning and at t time, respectively.

2.4 Characterization

The crystallite and morphology of Ag_3PO_4 NPs and Au@ Ag_3PO_4 NPs were characterized field-emission scanning electron microscopy (FE-SEM) (SEM 4500-Quanta), energy-dispersive X-ray (EDX) analysis, and X-ray diffraction spectra (XRD) measurements were performed on a Siemens Powder (X-500 instrument) using Cu $K\alpha$ radiation (40 kv), studies were conducted with Cu $K\alpha$ ($\lambda=1.54 \text{ \AA}$) at 45 kV voltage and 40 mA current. The scan rate, step size and 2θ range of the samples were 0.1 deg/s , 0.013° and $10\text{-}90^\circ$. Spectrophotometer type JENWAY 6700, Perkin-Elmer lambda 25 has been used.

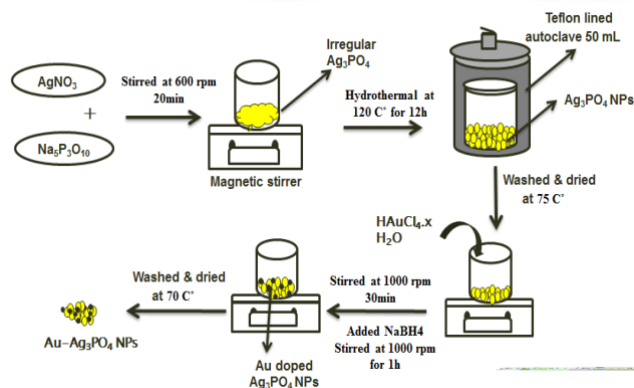


Fig 1. Schematic illustration for the synthesis of all process.

3. RESULT AND DISCUSSION

3.1 Characterization of Ag_3PO_4 NPs and Au@ Ag_3PO_4 NPs

The structural characterization and phase conformation analysis of the synthesized of undoped Ag_3PO_4 NPs and Au@ Ag_3PO_4 NPs photocatalyst samples were confirmed using XRD diffraction patterns, as shown in Fig. 2. The XRD diffraction peaks for undoped Ag_3PO_4 NPs could be readily indexed to the body-centred cubic structure of Ag_3PO_4 (JCPDS No. 06-0505) (Ma et al., 2014); and the diffraction pattern of undoped Ag_3PO_4 NPs indicates eight planes, which indexed to (110), (200), (210), (211), (222), (320), (321), and (520). However, In case of Au@ Ag_3PO_4 NPs samples, four different peaks were detected at 38.16° , 34.45° , 65.1° , and 82.3° , which could be well indexed to the (111), (200), and (220) crystal planes, respectively, indicating that Au has been successfully loaded onto silver phosphate NPs (JCPDS No. 01-1174) (Sun, Dong, & Wang, 2004). The existence of the four defined peaks confirmed the distribution of the Au metal in the Ag_3PO_4 NPs, also no other and broad peak indicated to the purity and crystalline of the catalyst and homogeneously formation between Au and silver phosphate.

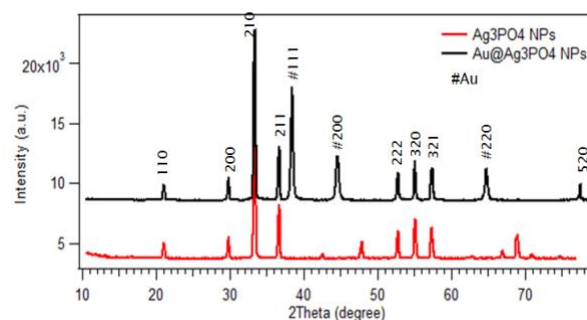


Fig 2. XRD patterns of pure Ag_3PO_4 nanoparticles and Au doped Ag_3PO_4 nanoparticles photocatalysts.

The morphology and composition of Ag_3PO_4 nanoparticles and $\text{Au}@Ag_3\text{PO}_4$ were detected via FESEM and EDX respectively, as shown in (Fig. 3 and 4). It can be seen that the Ag_3PO_4 NPs with particle size 747.81 nm to 800 nm at 12 h of hydrothermal reaction and regular spherical morphology and homogenously were formed (Fig. 3A). In the figure 2B, the present research work the doped Ag_3PO_4 NPs nanoparticles have exhibited grain sizes varying from 96.77 nm to 100 nm, which has homogenous meso pores net, as well the morphology has improved to a regular pattern as the Au noble metal is doped and the crystallite is increased, therefore the surface area of the whole prepared catalyst well be increase, it make the performance of the Photocatalytic degradation of dyes well increase. The variation in crystallite size of doped noble metals may be explained by the agglomeration of NPs. In Au doped Ag_3PO_4 sample more agglomeration are obtained.

The EDX spectrum in Fig. (4A, B) consists of corresponding peaks for P, Ag, O, and Au ions and it confirms the doped of Au noble metal ion in the prepared samples, it is worth mentioning that the presence of oxygen is due to the hydroxyl functionalized on the surface which makes nanoparticles soluble in water and also there were no other impurity peaks were found in the spectrum reveals the purity of the synthesized Ag_3PO_4 NPs.

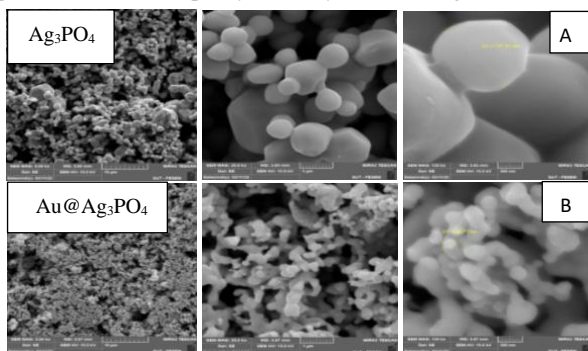


Fig. 3. Field emission scanning electron microscopy (FE-SEM) at different magnification of (A) Silver phosphate NPs(747.81nm) (B) gold doped Silver phosphate NPs(96.77nm).

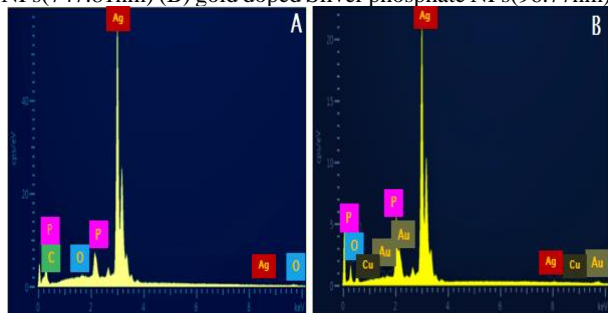


Fig. 4. EDX spectra of (A) silver phosphate NPs (B) gold doped Silver phosphate NPs.

Fig. 5(a) demonstrates the absorbance of Au doped Ag_3PO_4 and pure Ag_3PO_4 NPs. For the undoped Ag_3PO_4 NPs revealed that no absorbance at wavelengths greater than 520 nm, while for Au doped Ag_3PO_4 there was some absorbance observed as a broad peak between 520-560 nm, which is attributed to the agglomeration of gold particles and corresponding localized surface plasmon resonance (LSPR) absorption.

This blue shift could be ascribed by the formation of new donor centers (Zheng, Song, Jiang, & Lian, 2012), and the formation of shallow levels or sub band inside the band gap due to the incorporation of doping ions Au^{3+} (Ryu, Lee, & White, 2003). These levels could act to capture electrons, which facilitates electronic transitions from the valance band to these levels and then to the conduction band, as well as preventing electron-hole pair recombination.

In addition, as shown in the Fig. 5(b) the band gap was estimated by Tauc's equation which shows the relationship among absorption coefficient and the incident photon energy of doped

and undoped Ag_3PO_4 NPs. The Tauc's equation is presented as below (Butler, 1977; Huang, Schlichthörl, Nozik, Grätzel, & Frank, 1997)

$$(\alpha h\nu)^2 = A(h\nu - E_g)^{n/2} \quad (2)$$

Where α is the absorption coefficient, A is a constant, and n depends on whether the transition semiconductor is indirect (n = 4) and direct (n = 1).

The E_g obtained for pure Ag_3PO_4 NPs is 2.39 eV, which is in good agreement with a previous reported paper (Zhao et al., 2014). The E_g values of the Au doped Ag_3PO_4 NPs was found to be 2.34 eV. The E_g values suggest absorbance in the visible region with longer wavelengths, which will be highly beneficial for photoinduced charge transfer from gold (Au) to Ag_3PO_4 and would ultimately lead to an increase of the photocatalytic performance of fabricated photocatalytic frameworks.

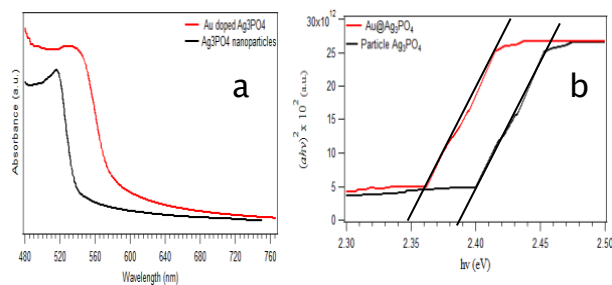


Fig. 5. (a) UV-vis absorption spectra of Au doped Ag_3PO_4 and pure Ag_3PO_4 NPs and (b) plots of $(\alpha h\nu)^2$ versus energy (h ν) of the band gap energy of Au doped Ag_3PO_4 and pure Ag_3PO_4 NPs.

3.2 Photo-catalytic degradation of fast green FCF dye

The photocatalytic activity and stability of Ag_3PO_4 NPs and $\text{Au}@Ag_3\text{PO}_4$ NPs were evaluated in the degradation of fast green FCF dye under visible light. As illustrated in Fig. 6 (a), $\text{Au}@Ag_3\text{PO}_4$ NPs shows significant enhancement in photocatalytic activity over Ag_3PO_4 NPs. the structure of fast green FCF dye is completely disintegrates at 15 min and the degraded efficiency remain constant due to completely reduction the dye to CO_2 and H_2O in the presence of $\text{Au}@Ag_3\text{PO}_4$ NPs, otherwise in the existence of undoped Ag_3PO_4 NPs it need approximately 55 min to partially degraded fast green dye, that is mean the noble metal Au lead to formation sub bands between valance and conduction band and the electron easily will transfer to conduction band, this leads to exhibits the highest photocatalytic activity and stability compared with undoped. In addition, as shown in the Fig 6 (b), the kinetics of fast green FCF degradation over the $\text{Au}@Ag_3\text{PO}_4$ NPs and Ag_3PO_4 NPs catalysts, the straight lines obtained in the kinetic assigned to a pseudo-first-order kinetics reaction with a simplified Langmuir-Hinshelwood model

$$\ln(C^0/C) = kt \quad (3)$$

Where k is reaction rate constant, C^0 and C are concentration of dye at initial and the reaction time. The rate constants (k) for fast green FCF degradation by $\text{Au}@Ag_3\text{PO}_4$ NPs and Ag_3PO_4 NPs catalysts under visible light were determined to be 0.182 and 0.063, min^{-1} , respectively. That is mean the degradation rate of fast green FCF by $\text{Au}@Ag_3\text{PO}_4$ NPs is ~ 3 times higher than that by undoped Ag_3PO_4 NPs. Finally in the Fig. 6 (c), reveals that the absorption features of fast green FCF dye in the presence of $\text{Au}@Ag_3\text{PO}_4$ NPs. The peak of dye at 625 nm is completely degrade FG dye in only 15 min, compare with undoped.

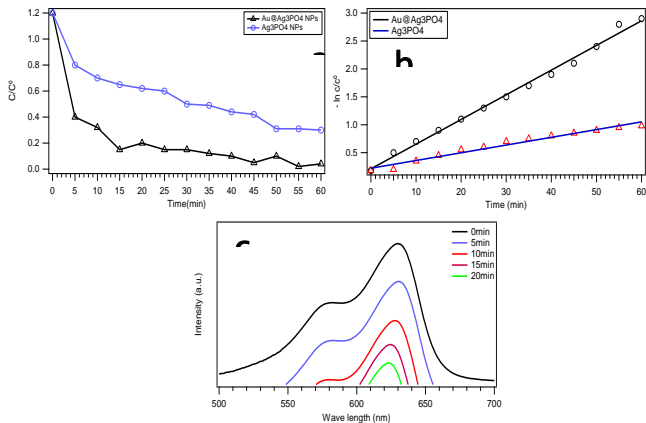


Fig. 6. (a) Photocatalytic activity of Ag₃PO₄ & Au@Ag₃PO₄ NPs of FG dye at different time.(b) the kinetic study of Ag₃PO₄ & Au@Ag₃PO₄ NPs for the photo degradation of FG dye (c) UV-Vis absorption spectra of FG dye (10mg/L,100mL) in the presence of Au@Ag₃PO₄ NPs as a catalyst at $\lambda = 625$ nm and pH=6.5.

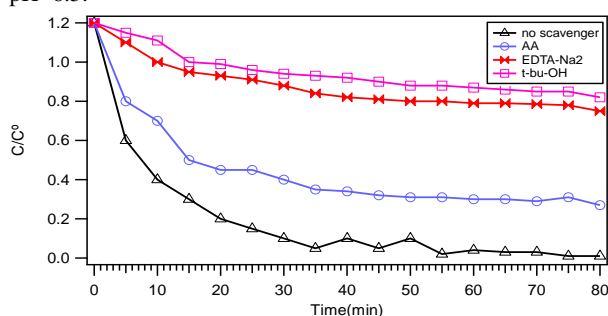


Fig. 7. Scavenger test of Au@Ag₃PO₄ NPs for fast green FCF degradation under visible light irradiation. AA, DETA, and t-BuOH, were scavengers for O₂^{•-}, h⁺ and •OH radicals, respectively.

3.3 Photo-catalytic mechanism Au@Ag₃PO₄ NPs

It is extensively known that the main active species (i.e O₂^{•-}, h⁺ and •OH) for oxidizing organic pollutants in the photocatalytic degradation process (Li et al., 2017). When surface of doped catalyst is irradiated by the UV-Visible light, transition of (e⁻) from valence band to the conduction band, however the photo-generated hole (h⁺) on the semiconductor valence band might oxidize hydroxyl molecule (OH⁻) in the solution to hydroxyl radical (•OH) and then it will oxidize the GF dye molecule or directly oxidize the GF dye molecule by photo-generated hole (h⁺) as shown in Fig. 8. In this experiment, three different types of scavengers are used to detect the active species, (i.e ascorbic acid (AA), disodium ethylenediaminetetraacetate (Na₂-EDTA) each (2mM) were scavengers for O₂^{•-} radical and h⁺ respectively, and tert-butanol (t-BuOH) as •OH radical) were employed. As shown in the figure (3), (t-BuOH) as •OH radical) were added to Photocatalytical system showed lesser photocatalytic activity comparing with AA and EDTA-2Na, suggesting that the •OH played the assisted role during the course of degradation reaction of fast green FCF; however, addition both of AA and EDTA-2Na in the system with the catalyst it lead to degraded FG rapidly. Therefore, this means that (•OH radical) shows a minor role in the photocatalytic reaction, but (O₂^{•-} radical and (h⁺) are the main active species in the degradation of FG dye by Au@Ag₃PO₄ NPs. As a result the order of creation rates of these species can be as follows: no scavenger > O₂^{•-} > h⁺ > •OH.

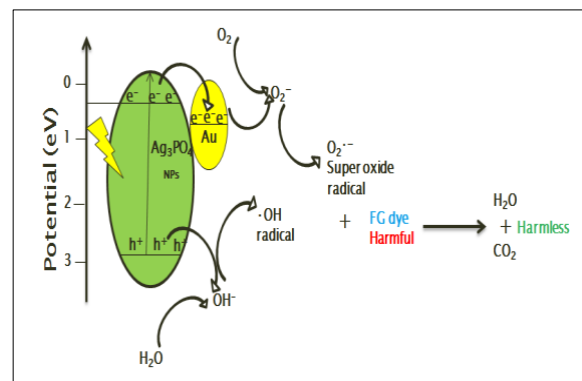


Fig. 8. The proposed mechanism of the Au@Ag₃PO₄ NPs as a Photo-catalyst in degradation of FG day.

4. CONCLUSION

In the present work, Ag₃PO₄ NPs were successfully designed and manufactured via hydrothermal method. Au@Ag₃PO₄ NPs were synthesized by chemical reduction method. In addition, the structure, morphology, composition and optical properties were determined by using XRD, FE-SEM, EDX and UV-Visible spectroscopy characterization techniques respectively. The obtained results indicate that the Au@Ag₃PO₄ NPs exhibit higher photocatalytic reduction performances of fast green FCF dye compared to the bare Ag₃PO₄ NPs photocatalyst under visible light illumination. Based on the Langmuir-Hinshelwood mechanism, a pseudo first-order kinetic model was demonstrated. Finally, these extremely sustainable features of the synthesized photocatalyst of Au doped Ag₃PO₄ NPs can be a new approach for the researchers to develop their applications in purpose of removal of different harmful and toxic pollutants under the clean energy of visible light

REFERENCES

- Alam, U., Fleisch, M., Kretschmer, I., Bahnemann, D., & Muneer, M. (2017). One-step hydrothermal synthesis of Bi-TiO₂ nanotube/graphene composites: an efficient photocatalyst for spectacular degradation of organic pollutants under visible light irradiation. *Applied Catalysis B: Environmental*, 218, 758-769.
- Anusha, M., & Arivuoli, D. (2013). High intense violet luminescence in fluorine doped zinc oxide (FZO) thin films deposited by aerosol assisted CVD. *Journal of Alloys and Compounds*, 580, 131-136. doi: DOI 10.1016/j.jallcom.2013.05.073
- Atacan, K., Güy, N., Ozmen, M., & Özacar, M. (2021). Fabrication of silver doped different metal oxide nanoparticles and evaluation of their antibacterial and catalytic applications. *Applied Surface Science Advances*, 6, 100156.
- Atacan, K., Özacar, M., & Özacar, M. (2018). Investigation of antibacterial properties of novel papain immobilized on tannic acid modified Ag/CuFe₂O₄ magnetic nanoparticles. *International journal of biological macromolecules*, 109, 720-731.
- Bauer, W., & Tomandl, G. (1994). Preparation of spherical TiO₂ particles by an emulsion method using TiCl₄. *Ceramics international*, 20(3), 189-193.
- Bouزيد, H., Faisal, M., Harraz, F. A., Al-Sayari, S. A., & Ismail, A. A. (2015). Synthesis of mesoporous Ag/ZnO nanocrystals with enhanced photocatalytic activity. *Catalysis Today*, 252, 20-26.
- Butler, M. (1977). Photoelectrolysis and physical properties of the semiconducting electrode WO₂. *Journal of Applied Physics*, 48(5), 1914-1920.
- CHENG, F., LIU, W.-s., Juan, W., & WANG, Y.-k. (2015). Research progress of Ag₃PO₄-based photocatalyst: Fundamentals and performance enhancement. *Transactions of Nonferrous Metals Society of China*, 25(1), 112-121.
- Dayana, P. N., Abel, M. J., Inbaraj, P., Sivaranjani, S., & Thiruneelakandan, R. (2021). Zirconium Doped Copper Ferrite (CuFe₂O₄) Nanoparticles for the Enhancement of

- Visible Light-Responsive Photocatalytic Degradation of Rose Bengal and Indigo Carmine Dyes. *Journal of Cluster Science*, 1-11.
- Downing, J. M., Ryan, M. P., & McLachlan, M. A. (2013). Hydrothermal growth of ZnO nanorods: The role of KCl in controlling rod morphology. *Thin Solid Films*, 539, 18-22. doi: DOI 10.1016/j.tsf.2013.04.131
- Faisal, M., Jalalah, M., Harraz, F. A., El-Toni, A. M., Khan, A., & Al-Assiri, M. (2020). Au nanoparticles-doped g-C₃N₄ nanocomposites for enhanced photocatalytic performance under visible light illumination. *Ceramics international*, 46(14), 22090-22101.
- Faisal, M., Khan, S. B., Rahman, M. M., Jamal, A., Akhtar, K., & Abdullah, M. (2011). Role of ZnO-CeO₂ nanostructures as a photo-catalyst and chemi-sensor. *Journal of Materials Science & Technology*, 27(7), 594-600.
- Faisal, M., Khan, S. B., Rahman, M. M., Jamal, A., Asiri, A. M., & Abdullah, M. (2011a). Smart chemical sensor and active photo-catalyst for environmental pollutants. *Chemical Engineering Journal*, 173(1), 178-184.
- Faisal, M., Khan, S. B., Rahman, M. M., Jamal, A., Asiri, A. M., & Abdullah, M. (2011b). Synthesis, characterizations, photocatalytic and sensing studies of ZnO nanocapsules. *Applied Surface Science*, 258(2), 672-677.
- Faisal, M., Tariq, M. A., & Muneer, M. (2007). Photocatalysed degradation of two selected dyes in UV-irradiated aqueous suspensions of titania. *Dyes and Pigments*, 72(2), 233-239.
- Farah, M. A., Ateeq, B., Ali, M. N., Sabir, R., & Ahmad, W. (2004). Studies on lethal concentrations and toxicity stress of some xenobiotics on aquatic organisms. *Chemosphere*, 55(2), 257-265.
- Guan, X., & Guo, L. (2014). Cocatalytic effect of SrTiO₃ on Ag₃PO₄ toward enhanced photocatalytic water oxidation. *Acs Catalysis*, 4(9), 3020-3026.
- Huang, S., Schlichthörl, G., Nozik, A., Grätzel, M., & Frank, A. (1997). Charge recombination in dye-sensitized nanocrystalline TiO₂ solar cells. *The Journal of Physical Chemistry B*, 101(14), 2576-2582.
- Ilican, S. (2013). Effect of Na doping on the microstructures and optical properties of ZnO nanorods. *Journal of Alloys and Compounds*, 553, 225-232.
- Karimi-Maleh, H., Kumar, B. G., Rajendran, S., Qin, J., Vadivel, S., Durgalakshmi, D., . . . Karimi, F. (2020). Tuning of metal oxides photocatalytic performance using Ag nanoparticles integration. *Journal of Molecular Liquids*, 314, 113588.
- Kathirvel, S., Pedaballi, S., Su, C., Chen, B.-R., & Li, W.-R. (2020). Morphological control of TiO₂ nanocrystals by solvothermal synthesis for dye-sensitized solar cell applications. *Applied Surface Science*, 519, 146082.
- Kumar, V. V., Gayathri, K., & Anthony, S. P. (2016). Synthesis of α -MoO₃ nanoplates using organic aliphatic acids and investigation of sunlight enhanced photodegradation of organic dyes. *Materials Research Bulletin*, 76, 147-154.
- Li, H., Peng, Z., Qian, J., Wang, M., Wang, C., & Fu, X. (2017). C Fibers@ WSe₂ Nanoplates Core-Shell Composite: Highly Efficient Solar-Driven Photocatalyst. *ACS applied materials & interfaces*, 9(34), 28704-28715.
- Long, Y., Lu, Y., Huang, Y., Peng, Y., Lu, Y., Kang, S.-Z., & Mu, J. (2009). Effect of C₆₀ on the photocatalytic activity of TiO₂ nanorods. *The Journal of Physical Chemistry C*, 113(31), 13899-13905.
- Ma, J., Zou, J., Li, L., Yao, C., Kong, Y., Cui, B., . . . Li, D. (2014). Nanocomposite of attapulgite-Ag₃PO₄ for Orange II photodegradation. *Applied Catalysis B: Environmental*, 144, 36-40.
- Nagaraju, G., Shivaraju, G., Banuprakash, G., & Rangappa, D. (2017). Photocatalytic activity of ZnO nanoparticles: synthesis via solution combustion method. *Materials Today: Proceedings*, 4(11), 11700-11705.
- Okafor, S. N., Obonga, W., Ezeokonkwo, M. A., Nurudeen, J., Orovwigho, U., & Ahiabuikwe, J. (2016). Assessment of the health implications of synthetic and natural food Colourants—A critical review. *Pharmaceutical and Biosciences Journal*, 01-11.
- Omer, A. M. (2008). Energy, environment and sustainable development. *Renewable and sustainable energy reviews*, 12(9), 2265-2300.
- Pathak, T. K., Swart, H., & Kroon, R. (2018). Structural and plasmonic properties of noble metal doped ZnO nanomaterials. *Physica B: Condensed Matter*, 535, 114-118.
- Rawat, J., Bijalwan, K., Negi, C., Sharma, H., & Dwivedi, C. (2021). Magnetically recoverable Au doped iron oxide nanoparticles coated with graphene oxide for catalytic reduction of 4-nitrophenol. *Materials Today: Proceedings*, 45, 4869-4873.
- Rycenga, M., Cobley, C. M., Zeng, J., Li, W., Moran, C. H., Zhang, Q., . . . Xia, Y. (2011). Controlling the synthesis and assembly of silver nanostructures for plasmonic applications. *Chemical reviews*, 111(6), 3669-3712.
- Ryu, Y., Lee, T., & White, H. (2003). Properties of arsenic-doped p-type ZnO grown by hybrid beam deposition. *Applied Physics Letters*, 83(1), 87-89.
- Sarina, S., Waclawik, E. R., & Zhu, H. (2013). Photocatalysis on supported gold and silver nanoparticles under ultraviolet and visible light irradiation. *Green chemistry*, 15(7), 1814-1833.
- Sharma, G., Bhogal, S., Naushad, M., Kumar, A., & Stadler, F. J. (2017). Microwave assisted fabrication of La/Cu/Zr/carbon dots trimetallic nanocomposites with their adsorptional vs photocatalytic efficiency for remediation of persistent organic pollutants. *Journal of Photochemistry and Photobiology A: Chemistry*, 347, 235-243.
- Sun, X., Dong, S., & Wang, E. (2004). Large-scale synthesis of micrometer-scale single-crystalline Au plates of nanometer thickness by a wet-chemical route. *Angewandte Chemie*, 116(46), 6520-6523.
- Vickers, N. J. (2017). Animal communication: when i'm calling you, will you answer too? *Current biology*, 27(14), R713-R715.
- Wang, F., Seo, J.-H., Li, Z., Kvit, A. V., Ma, Z., & Wang, X. (2014). Cl-Doped ZnO Nanowires with Metallic Conductivity and Their Application for High-Performance Photoelectrochemical Electrodes. *ACS Applied Materials & Interfaces*, 6(2), 1288-1293. doi: 10.1021/am405141s
- Wang, P., Huang, B., Dai, Y., & Whangbo, M.-H. (2012). Plasmonic photocatalysts: harvesting visible light with noble metal nanoparticles. *Physical Chemistry Chemical Physics*, 14(28), 9813-9825.
- Wategaonkar, S., Pawar, R., Parale, V., Nade, D., Sargar, B., & Mane, R. (2020). Synthesis of rutile TiO₂ nanostructures by single step hydrothermal route and its characterization. *Materials Today: Proceedings*, 23, 444-451.
- Yi, Z., Ye, J., Kikugawa, N., Kako, T., Ouyang, S., Stuart-Williams, H., . . . Li, Z. (2010). An orthophosphate semiconductor with photooxidation properties under visible-light irradiation. *Nature Materials*, 9(7), 559-564.
- Zhao, J., Ji, Z., Xu, C., Shen, X., Ma, L., & Liu, X. (2014). Hydrothermal syntheses of silver phosphate nanostructures and their photocatalytic performance for organic pollutant degradation. *Crystal Research and Technology*, 49(12), 975-981.
- Zheng, J., Song, J., Jiang, Q., & Lian, J. (2012). Enhanced UV emission of Y-doped ZnO nanoparticles. *Applied Surface Science*, 258(18), 6735-6738.